Journal of Pharmaceutical and Biomedical Analysis 149 (2018) 308–317

Contents lists available at ScienceDirect

Journal of Pharmaceutical and Biomedical Analysis

journal homepage: www.elsevier.com/locate/jpba

Comprehensive phospholipid and sphingomyelin profiling of different brain regions in mouse model of anxiety disorder using online two-dimensional (HILIC/RP)-LC/MS method

Róbert Berkecz[a,*], Ferenc Tömösi[a], Tímea Körmöczi[a], Viktor Szegedi[b], János Horváth[b], Tamás Janáky[a]

[a] Department of Medical Chemistry, Faculty of Medicine, University of Szeged Dóm tér 8, H-6720, Szeged, Hungary
[b] Department of Physiology, Anatomy and Neuroscience, University of Szeged, Közép fasor 52, H-6726, Szeged, Hungary

ARTICLE INFO

Article history:
Received 11 September 2017
Received in revised form 29 October 2017
Accepted 30 October 2017
Available online 8 November 2017

Keywords:
Phospholipid
Sphingomyelin
Brain
2D-LC/MS
Lipidomics
Anxiety disorder

ABSTRACT

A novel online system including two-dimensional liquid chromatography coupled to high-resolution mass spectrometry (2D-LC/MS) was developed and applied for comprehensive phospholipid (PL) and sphingomyelin (SM) profiling of dorsal hippocampus (DHPC), ventral (VHPC) and prefrontal cortex (PFC) brain regions in a mouse model of anxiety disorder. In the first dimension, lipid classes were distinguished by hydrophilic interaction liquid chromatography (HILIC), while the second dimensional separation of individual PL and SM species was achieved by reversed-phase (RP) chromatography. For the enrichment of lipid species in diluted HILIC effluent, two RP trapping columns were used separately. The developed fully-automated 2D method allowed the quantitative analysis of over 150 endogenous PL and SM species in mouse brain regions within 40 min. The developed method was applied in a pilot study, which aimed to find alteration of PL and SM composition in a mouse model of anxiety disorder. In the case of 37 PL and SM species, significant differences were observed between high anxiety-related behavior (AX) and low anxiety-related behavior (nAX) mice. In mice having elevated anxiety, the most typical trend was the downregulation of PL species, in particular, in VHPC.

1. Introduction

Non-targeted analysis of biomolecules is an important trend in the field of omics such as proteomics, genomics, transcriptomics and metabolomics. Lipidomics, an emerging field of metabolomics, aims for the comprehensive analysis of lipids in cells, tissues and biological fluids and monitors the lipid responses to various external or internal effects/events [1–4]. Chemically, eight lipid categories are known, namely, fatty acyls (FA), glycerolipids, saccharolipids, polyketides, sterol lipids, prenol lipids, sphingolipids and PLs. According to the polar head group of PLs, phosphatidylcholine (PC), phosphatidylethanolamine (PE), phosphatidylinositol (PI), phosphatidylserine (PS), phosphatidylglycerol (PG) and phosphatidic acid (PA) classes are distinguished [5,6].

Nowadays, the coupling of LC to MS is one of the most powerful and widespread techniques to analyze lipid molecular species in complex samples. The main advantages of the use of this hyphenated technique, compared to direct infusion called "shotgun" methods, are its ability to distinguish isomers (isobars) and obtain higher sensitivity of low-abundance lipids owing to reduced ion suppression effect [7–9]. In LC, lipids are usually separated by RP, HILIC or normal phase (NP) methods. In RP-LC, the retention behavior of lipids are in correlation with the equivalent carbon number, while in the case of NP-LC and HILIC, the retention of lipid classes depends on the hydrophilic properties of the polar head group [4,10,11]. The solvent system used in NP-LC usually provides low ionization efficiency in MS detection, while RP-LC and HILIC mobile phases are MS compatible and result in good ionization [12].

Abbreviations: 1D, one-dimensional; 2D-LC/MS, two-dimensional liquid chromatography coupled to high resolution mass spectrometry; AGC, automatic gain control; AX, anxiety-related behavior; C18, octadecylsilyl; DHPC, dorsal hippocampus; FA, fatty acyl; HILIC, hydrophilic interaction liquid chromatography; IS, internal standard; LPL, lysophospholipid; ME, matrix effect; nAX, low anxiety-related behavior; NP, normal phase; OPLS-DA, orthogonal partial least square discriminant analysis; PA, phosphatidic acid; PC, phosphatidylcholine; PE, phosphatidylethanolamine; PFC, prefrontal cortex; PG, phosphatidylglycerol; PI, phosphatidylinositol; PL, phospholipid; PS, phosphatidylserine; RE, extraction recovery; RP, reversed-phase; R_S, chromatographic resolution; SEM, standard errors; SM, sphingomyelin; VHPC, ventral hippocampus.

* Corresponding author.
E-mail address: berkecz.robert@med.u-szeged.hu (R. Berkecz).

https://doi.org/10.1016/j.jpba.2017.10.043
0731-7085/

Lipidomics deals with large sample complexity; therefore, one-dimensional (1D) chromatographic separation can provide limited selectivity for lipid species in any chromatographic mode resulting in difficulties in identification and quantification [13]. The combination of different LC modes could provide a number of possibilities to improve separation of lipid molecular species through enhanced chromatographic resolution and higher peak capacity. Two connected orthogonal LC modes, such as NP-LC or HILIC or silver-ion chromatography (for nonpolar lipids) with RP-LC, either online or offline, have already been used in lipidomics. [13–21]. The main benefit of offline 2D techniques is that the chromatographic conditions in both dimensions can be completely optimized, which helps to improve the separation of lipid species. On the other hand, it is not automated and additional sample preparation steps, such as fraction collection, evaporation of mobile phase, reconstitution and rerun in second dimension, make this method time-consuming and labor-intensive and may result in degradation of the sample. Online 2D techniques, in turn, give an opportunity for the development of completely automated measurements with a low risk of sample loss and degradation. However, this technique provides compromising chromatographic resolution in the first and/or second dimension due to the synchronization of both dimensions and requires a high level of instrumentation [14,16,19].

Although anxiety disorders are among the most widespread affective diseases, their pathogenesis is still poorly understood. The generation and regulation of the sustained anxious mood are a complex process, in which several brain regions (also referred to as the fear circuitry) are involved in the generation of fear. Key areas of the brain are the medial PFC and VHPC, sharing a monosynaptic connection, which functionally interacts during innate anxiety tasks [22–25]. It is the VHPC, which is also interconnected with the amygdala and the entorhinal cortex and mediates the effect of glucocorticoids on anxiety in the brain [26–29]. The use of animal models of anxiety disorder may help to understand human disorders. Two mouse strains with extremes in their anxiety-related phenotype have been established by using an intra-strain and a selective bidirectional inbreeding approach that led to an accumulation of genetic material associated with the respective anxiety phenotype. Our group has previously studied neurophysiological and brain proteome differences in AX and nAX mouse strains and now we present our lipidomics results on this animal model [30,31].

The main goal of this study was the development of a new, online 2D-LC/MS method for the characterization of the PL and SM composition of different brain regions of nAX and AX mice. Comprehensive lipidomics analysis was achieved by separation of lipid classes by HILIC chromatography (first dimension) followed by reversed-phase chromatography (second dimension) on a UHPLC column packed with fully porous sub–2 μm C18 particles to separate lipids species. The identification of brain polar lipid species was based on the retention times in both dimensions, the accurate *m/z* values and isotope patterns of the detected ions ($[M-H]^-$ or $[M+HCOO]^-$, depending on PL classes). Quantification of PL species identified was carried out by using internal standards.

2. Materials and methods

2.1. Animals and tissue samples

Inbred mouse strains having either AX or nAX were bred in our animal facility. These strains were originally developed at EGIS Pharmaceuticals PLC (Budapest, Hungary) by bidirectional inbreeding based on anticipatory anxiety [30]. 2.5–3-month-old male mice were housed individually under a light/dark 12-h cycle (lights on at 08:00) at 24 ± 1 °C temperature giving *ad libitum* access to food and water. For the experiments, 80–85th generations were used. The mice were sacrificed, their brains were rapidly removed and PFC, VHPC and DHPC regions were dissected. The wet samples were weighed, snap-frozen in liquid nitrogen and stored at −80 °C before homogenization. The study was in compliance with EU directive 2010/63/EU and was approved by the regional Station for Animal Health and Food Control under Project License XXXI/2012.

2.2. Chemicals and standards

1-Heptadecanoyl-2-hydroxy-*sn*-glycero-3-phosphate (sodium salt) (**LPA 17:0**), 1,2-dimyristoyl-*sn*-glycero-3-phosphate (sodium salt) (**PA 14:0/14:0**), *N*-lauroyl-D-erythro-sphingosylphosphorylcholine (**SM d18:1/12:0**), 1-myristoyl-2-hydroxy-*sn*-glycero-3-phospho-(1′-rac-glycerol) (sodium salt) (**LPG 14:0**), 1,2-diheptadecanoyl-*sn*-glycero-3-phospho-(1′-rac-glycerol) (sodium salt) (**PG 17:0/17:0**), 1-nonadecanoyl-2-hydroxy-*sn*-glycero-3-phosphocholine (**LPC 19:0**), 1,2-dimyristoyl-*sn*-glycero-3-phosphocholine (**PC 14:0/14:0**), 1,2-dimyristoyl-*sn*-glycero-3-phospho-L-serine (sodium salt) (**PS 14:0/14:0**), 1-myristoyl-2-hydroxy-*sn*-glycero-3-phosphoethanolamine (**LPE 14:0**), and 1,2-dimyristoyl-sn-glycero-3-phosphoethanolamine (**PE 14:0/14:0**) were purchased from Avanti Polar Lipids (Alabaster, USA) and used as internal standards (IS). Water, methanol, acetonitrile, ammonium formate (all LC–MS grade), *n*-hexane, and chloroform (HPLC grade) were purchased from VWR (Radnor, USA). LC–MS-grade 2-propanol was purchased from Fluka (Buchs, Switzerland) and acetone (GC–MS grade) was from MERCK (Darmstadt, Germany).

2.3. Sample preparation

The weighed brain samples were placed into 1.7 mL microcentrifuge tubes and an appropriate volume of ammonium formate buffer (50 mM) were added in order to obtain 5 μg/μL concentration of each homogenate. The samples were individually sonicated with a BioLogics Model 150VT ultrasonic homogenizer (BioLogics Inc, Manassas, VA, USA) for 1 min using full power setting with a 50% pulse on the micro-tip probe.

Extraction of lipids from brain homogenate was performed according to a slightly modified Folch procedure [32]. Prior to extraction, 10 μL brain homogenate was spiked with 10 μL lipid standard mixture (100 pmol/μL **PC 14:0/14:0**, 100 pmol/μL **LPC 19:0**, 50 pmol/μL **PE 14:0/14:0**, 30 pmol/μL **LPE 14:0**, 5 pmol/μL **PG 17:0/17:0**, 5 pmol/μL **LPG 14:0**, 50 pmol/μL **PA 14:0/14:0**, 50 pmol/μL **LPA 17:0**, 50 pmol/μL **PS 14:0/14:0** and 125 pmol/μL **SM d18:1/12**). After vortex mixing, 5 μL of butylated hydroxytoluene (2 mg/mL in ethanol) and 450 μL of chloroform/methanol (2:1, v/v) were added, followed by vortex mixing. The mixture was shaken for 15 min at room temperature. After the addition of 115 μL of ammonium formate (50 mM), the sample was vortexed for 20 s. Upon 5 min of incubation at room temperature, the sample was centrifuged at 1000 g for 10 min 200 μL of the lower phase was collected, and the upper phase was re-extracted with 200 μL of chloroform. After centrifugation, 300 μL of the lower phase was combined with the first portion of organic phase and dried by a nitrogen stream at ambient temperature. For 2D-LC/MS measurements, the dried extracts were reconstituted in 100 μL chloroform/methanol (2:1, v/v) mixture.

2.4. 2D-LC/MS conditions

2D-LC/MS analysis was performed by using a Waters Acquity I-Class UPLC™ system (Waters, Manchester, UK), equipped with two binary solvent managers, an auto-sampler and a column manager with two six-port, two-position automatic switching valves. The

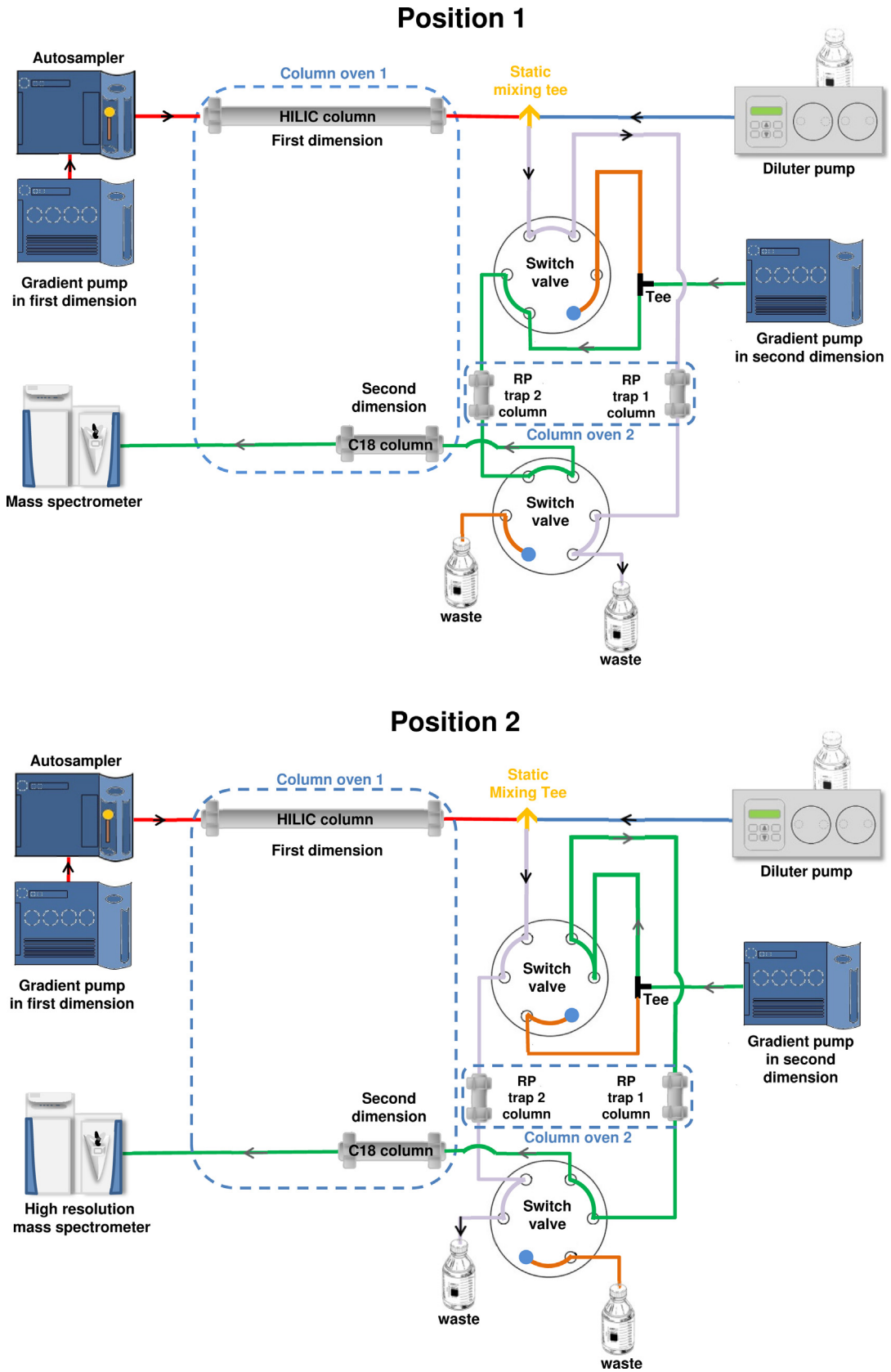

Fig. 1. Flow scheme of the established 2D-LC/MS system in both valve positions: Position 1 and Position 2.

eluent of the first-dimensional HILIC column was diluted using a HITACHI L-7100 pump (Hitachi, Tokyo, Japan) and a high-pressure static mixing tee (IDEX, Oak Harbor, WA, USA). The first and second dimensional analytical columns were thermostated in the column manager of the UPLC system, while for the enrichment columns, a L-7350 LaChrom column oven (Merck, Darmstadt, Germany) was

used. The ultrahigh-performance liquid chromatography (UPLC) system was coupled to Thermo Scientific Q Exactive Plus hybrid quadrupole-Orbitrap (Thermo Fisher Scientific, Waltham, MA, USA) mass spectrometer. The experimental configuration of our online 2D-LC/MS system is illustrated in Fig. 1.

In the 2D-LC/MS system, the first- and second-dimension columns were connected through two six-port valves and two Luna C18 (20 × 2.0 mm, 5 μm, 100 Å, Phenomenex) enrichment columns (Fig. 1). By the scheduled switching of the six-port valves, the diluted mobile phase from the HILIC column in first dimension was trapped on C18 enrichment column, while the trapped compounds on the other C18 enrichment column were analyzed in the second dimension in sync (Table 1). To prevent the elution of lipid species from the enrichment columns during the trapping process, the diluter pump delivered 5 mM ammonium formate eluent at a flow rate of 0.6 mL/min into the static mixing tee, which was connected after the HILIC column and in front of the first six-port valve. The trap columns were maintained at 50 °C.

Fig. 1 demonstrates the schematic representation of our 2D-LC/MS system in "Position 1" arrangement, where the "RP trap 1" column was first used to enrich analytes from the diluted effluent of the HILIC column. The system was kept in this configuration for 8 min. Then switching valves were turned into "Position 2" as shown in Fig. 1. The diluted mobile phase from the HILIC column was then trapped on the "RP trap 2" column and, at the same time, the analytes trapped on the "RP trap 1" column were washed onto and separated on the second-dimensional RP analytical column. The complete schedule of event times is detailed in Table 1. The number of valve events was odd (5), which would have resulted in the same initial valve positions in consecutive analysis. Namely, in the first HILIC effluent trapping section (0–8 min), the eluted analytes of the given measurement would have enriched on the same trap column that was used in last section of previous measurement. Therefore, to prevent the undesired "double trapping" on the enrichment columns, two methods with the same LC and MS parameters had to be established, which differed only in the order of valve positions (Table 1). The two methods had to be strictly alternated in sample sequence. Components that trapped in the washing and re-equilibration steps of the HILIC column (32–40 min) were detected in the first RP-LC run of the following sample but were ignored in data evaluation (Fig. 2).

Lipid classes were separated in the first dimension after injecting 10 μL of sample/standard on a Kinetex HILIC column (150 × 2.1 mm, 2.6 μm, 100 Å, Phenomenex) using programmed gradient of eluent *A* (50 mM ammonium formate solution) and eluent *B* (acetone) (Table 1). The flow rate of the mobile phase and the temperature were kept, respectively, at 0.4 mL/min and 50 °C during the analysis. The injector needle was washed with hexane-2-propanol-water (2:2:0.1, v/v/v) mixture after each injection.

In the second dimension, eluent *A* and *B* were water/acetonitrile (50:50, v/v) and water/acetone (5:95, v/v), respectively, both containing 5 mM ammonium formate. The mobile phase washed the substances trapped on a given C18 enrichment column onto an Acquity UPLC BEH C18 analytical column (2.1 × 50 mm, 1.7 μm, 130 Å, Waters) at a flow rate of 0.4 mL/min. The column was maintained at 50 °C. The gradient programs of both dimensional are detailed in Table 1.

The mass spectrometer was operated in the negative-ion mode using a heated ESI source with the following conditions: capillary temperature 250 °C, S-Lens RF level 50, spray voltage 2.5 kV, sheath gas flow 45, sweep gas flow 2 and auxiliary gas flow 10, and full scan with a mass range of 100–1000 and a resolution of 35,000. The automatic gain control (AGC) setting was defined as 3×10^6 charges and the maximum injection time was set to 100 ms.

The LC system was controlled by MassLynx 4.1 SCN 901 (Waters, Milford, MA, USA). The control of MS system and MS data acquisition were conducted by the Xcalibur™ 4.0 software (Thermo Fisher Scientific, Waltham, MA).

2.5. Data processing

The alignment of retention times, peak picking, deconvolution, determination of peak area, as well as preliminary identification using LipidBlast database were performed from raw data by Progenesis QI (Nonlinear Dynamics, Newcastle, United Kingdom) [33]. Then, the processed data including peak area, *m*/*z* value, and retention time were imported into Microsoft Excel software for normalization of the peak areas, which was based on calculation of the analyte/IS peak area ratios. Identification of lipid species was accomplished via accurate mass (<3 ppm) database searching of LIPID MAPS and our homemade database built on our own measurements, literature sources and the prediction of retention times based on retention behavior of PL classes and PL species in both dimensions [6,34–39].

Multivariate data analysis of data including the normalized peak area and the abbreviation of the obtained identified lipids was performed by SIMCA software 14.1 (Umetrics, Umeå, Sweden). The obtained results of the orthogonal partial least square discriminant analysis (OPLS-DA) and the corresponding S-plots allowed the prediction of significant features (potential biomarkers) of which the alteration was in relation to the AX mouse model. Box plots and column diagrams with standard errors (SEM) were used to illustrate the data and the differences between the nAX and AX mice. These were assessed with *t*-test using GraphPad Prism 5 statistical software (GraphPad Software, Inc., La Jolla, CA, USA).

3. Results and discussion

3.1. Coupling of HILIC and RP-LC in 2D/LC

Several chromatographic parameters, such as column length, mobile phase composition, types and concentration of mobile phase additives, column temperature, gradient steepness and flow rate were investigated both in the first HILIC and the second RP-LC dimensions.

During optimization of HILIC, 100 mm and 150 mm length narrow-bore columns (2.1 mm) with porous shell particles were compared, and the latter was selected for further optimization to obtain better separation of PL classes. To achieve this goal, methanol, acetonitrile and acetone were tested as the organic component of the mobile phase. The application of acetone resulted in the highest retention and improved chromatographic resolution, in particular, for PCs and SMs, thus it was selected in the final method. In HILIC mode, the concentration of water in the mobile phase has a significant influence on the retention mechanism and the reproducibility of retention time by establishing of a water-enriched layer of semi-stagnant eluent on the stationary phase [40,41]. The minimum water content of the mobile phase was determined to be 3% (v/v) for the reproducible retention of lipids. The chromatographic behavior of the analytes is influenced by the type and concentration of the mobile phase modifiers. The volatile and MS-compatible ammonium formate was selected and added at 50 mM concentration to water for preparation of eluent *A*. In order to improve the trapping efficiency, the flow rate in first dimensional separation and the diluter pump had to be harmonized. Usually, the application of low flow rate in the first dimension promotes trapping efficiency of the analytes. However, it resulted in serious peak broadening in our case, thus as an optimum flow rate of 0.4 mL/min was selected. Lipid profiling of mouse brain extract with optimized HILIC chromatography is shown in Fig. 2(A). 11 PL classes, specifically, PG, PI, LPG, LPI, PE, PS, LPE, PC, PA, SM and LPC,

Table 1
The detailed gradient program and valve events of final 2D-LC/MS method.

First dimension (HILIC)			Valve position		Second dimension (RP-LC)		
Lipid classes	Retention time [min]	Solvent B [%]	Method 1	Method 2	Lipid species	Retention time [min]	Solvent B [%]
nonpolar lipids	0.0	97	1	2		0.0	30
FA						2.0	95
LPG						5.0	95
PG						5.1	30
						8.0	30
LPI			2	1	nonpolar lipids	8.0	30
PI					FA	10.0	95
PE					LPG	13.0	95
					PG	13.1	30
						16.0	30
LPE			1	2	LPI	16.0	30
PC					PI	18.0	95
PS					PE	21.0	95
						21.1	30
						24.0	30
PC			2	1	LPE	24.0	30
PS					PC	26.0	95
SM					PS	29.0	95
LPC	30.0	82				29.1	30
PA	31.0	50				32.0	30
			1	2	PC	32.0	30
	35.0	50			PS	34.0	95
	35.5	97			SM	37.0	95
					LPC	37.1	30
	40.0	97			PA	40.0	30

were distinguished within 40 min. Identification of these classes was performed in a separate 1D experiment by the application of the method detailed above. For analysis of lipid species in the second dimension, the eluate of the HILIC chromatography was divided into five fractions with 8 min of retention time windows, as demonstrated in Fig. 2(A).

By the use of reversed-phase C18 stationary phase, the retention and separation mechanism of lipids are based on the lengths of fatty acyl (or alkyl) chains and the number and the position of double bonds [4], which allow the discrimination of lipid species within the same class. For the separation of lipid species in second dimension, an Acquity UPLC BEH C18 micro-bore column with a particle size of 1.7 μm was selected. In order to achieve appropriate separation of lipid species within lipid classes at proper system pressure, flow rate and to get high ionization efficiency, a careful selection of the mobile phase was also needed. The use of water/acetonitrile (50:50, v/v) as A eluent and water/acetone (5:95, v/v) as B eluent (both containing 5 mM ammonium formate) proved to be a good compromise in point of view of system pressure, retention, selectivity and ionization efficiency of the analytes. For obtaining appropriate retention and chromatographic resolution within the 8-min runtime including washing and re-equilibration of the column, the temperature of C18 column, the flow rate and the gradient steepness were adjusted. In case of all lipid fractions, same RP gradient program was used in order to produce same retention time for those lipid species which were present in two HILIC fractions (e.g. PCs).In this way, the same chromatographic and mass spectrometric conditions were guaranteed for these species, which is a requirement for appropriate quantitative analysis combining peak species eluting in two consecutive fractions.

The collection/trap of analytes from the eluate of the first-dimensional column in a 2D-LC system is usually performed by the application of loop(s) or trap column(s) [13–21]. For the enrichment of the analytes in a loop, the mobile phase should be evaporated by the use of vacuum and temperature modulation. In the case of trap column, especially in highly orthogonal separation (e.g. NP × RP or HILIC × RP), the solvent strength of the effluent of first-dimensional column should be adjusted to retain analytes on the enrichment column. Using HILIC × RP-LC combination, we did not have to reckon on the solvent incompatibility problem, which is known in NP-LC × RP-LC methods. Acetone, applied as eluent *B* in HILIC mode, is a strong eluent in RP mode; therefore, it had to be diluted with a solvent with a very low eluting power in RP mode. An aqueous solution of ammonium formate (5 mM) was chosen for this purpose. The flow rate ratio of the HILIC mobile phase and the diluting solvent was critical for the appropriate retention of lipid species on the trap columns, especially at the beginning of analysis, when the effluent of HILIC column had high organic concentration. The effect of flow rate of the diluting eluent on the retention was investigated in the range 0.2–1 mL/min. A flow rate of 0.6 mL/min for the diluting eluent was the best compromise considering sufficient trapping of lipid species and proper system pressure.

3.2. Evaluation of extraction recovery and matrix effect

Prior to analysis, the enrichment of PLs through removal of the polar matrix is a crucial step to obtain reliable results. The determination of extraction recovery (RE) and matrix effect (ME) could help to decide whether an analytical method is feasible for quantitative analysis. The RE and ME of the developed method were determined by using 10 lipid class standards in accordance with the procedure of Matuszewski et al. and Cappiello et al. [42,43]. According to data on Fig. S1, the RE and ME of standard lipid species were reproducible and comparable. The high mean values of RE (above 85%) and repeatabilities for all lipid standards suggest that our extraction method is well established.

The matrix effect values ranged from 63.0 to 88.0%, which, because of the complexity of brain tissue, is an acceptable range. ME was below 100% for all standards examined indicating the lack of ionization enhancement during MS detection.

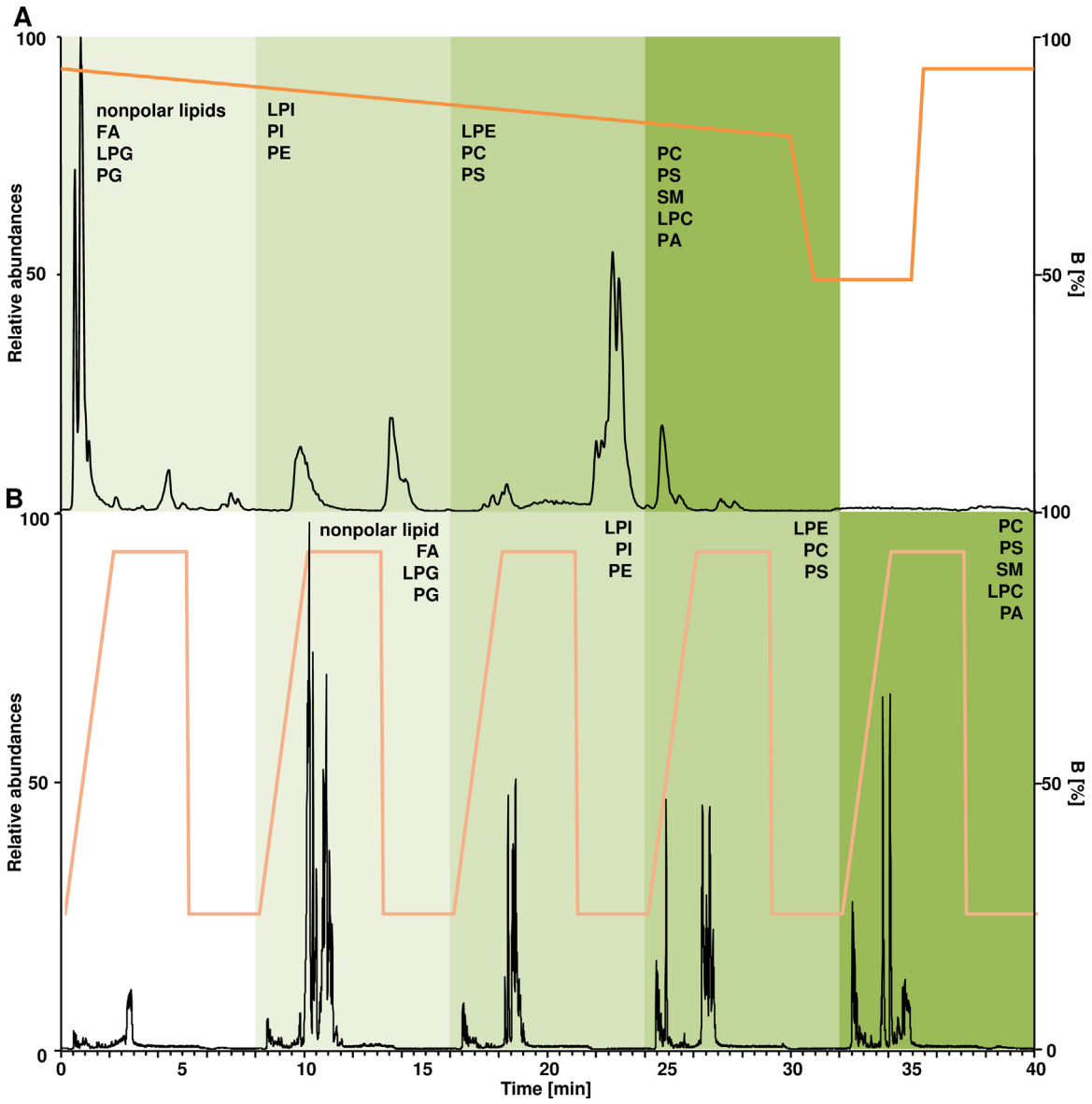

Fig. 2. Base peak chromatogram of PLs in VHPC of nAX mouse was detected by negative mode with 1D-HILIC method (A) and 2D-LC/MS method (B). Orange lines indicate the gradient LC profile in 1D and 2D measurements. (For interpretation of the references to colour in this figure legend, the reader is referred to the web version of this article.)

3.3. Identification and quantification of PLs in mouse brain regions

As shown in Fig. 2, HILIC was employed to differentiate PL classes in the first-dimensional run. The effluent obtained in the first dimension was divided into five fractions in order to separate individual PL species within classes according to the fatty acyl chain lengths and the number of double bonds using RP mode. The enhanced chromatographic resolution and higher peak capacities obtained by the 2D method is illustrated through the example of **PE 36:1**, **PE 36:2**, **PE 36:3**, **PE 34:4** and **PE 35:5** on Fig. 3, by presenting extracted ion chromatograms (negative ions) of HILIC/MS (**A**) and 2D-LC/MS (**B**). The advantage of 2D-LC/MS is demonstrated on Fig. 3(B) showing baseline separation of trapped phosphatidylethanolamine species. In lysophospholipids (LPLs), the fatty acyl chains are attached at either the sn-1 or sn-2 position of the glycerol backbone [4]. In several cases, separation of these isomers in LPI, LPE and LPC classes can be observed (Table S1).

Table S1 lists 151 endogenous PLs and SMs (3 LPG, 7PG, 5 LPI, 13 PI, 35 PE, 14 LPE, 37 PC, 11 PS, 8 SM, 14 LPC and 4 PA), which were identified by using our method in mouse brain regions. For quantitative analysis of the identified lipid molecules, the peak area of each individual lipid species was corrected by the corresponding internal standard. Relevant chromatographic and MS data along with the relative abundance of particular lipid species within classes determined in different brain regions (DHPC, VHPC and PFC) are presented in Table S1. Our results support the finding that nervous tissues contain high amounts of plasmanyl and plasmenyl PLs [44]. Fig. 4 illustrates the distribution of brain PL species containing acyl, alkyl ether and vinyl ether side chains within lipid classes. Plasmalogens and ether analogs were decisively present in PE and PC classes.

3.4. Comparing lipid profiles in the brain of nAX and AX mice

Seventeen mice from two strains were involved in the pilot study, 9 with low anxiety-related behavior and 8 with high anxiety-related behavior. Normalized peak areas of all identified lipid species in DHPC, VHPC and PFC of nAX and AX mice were statistically evaluated using the SIMCA (multivariate data analysis) and

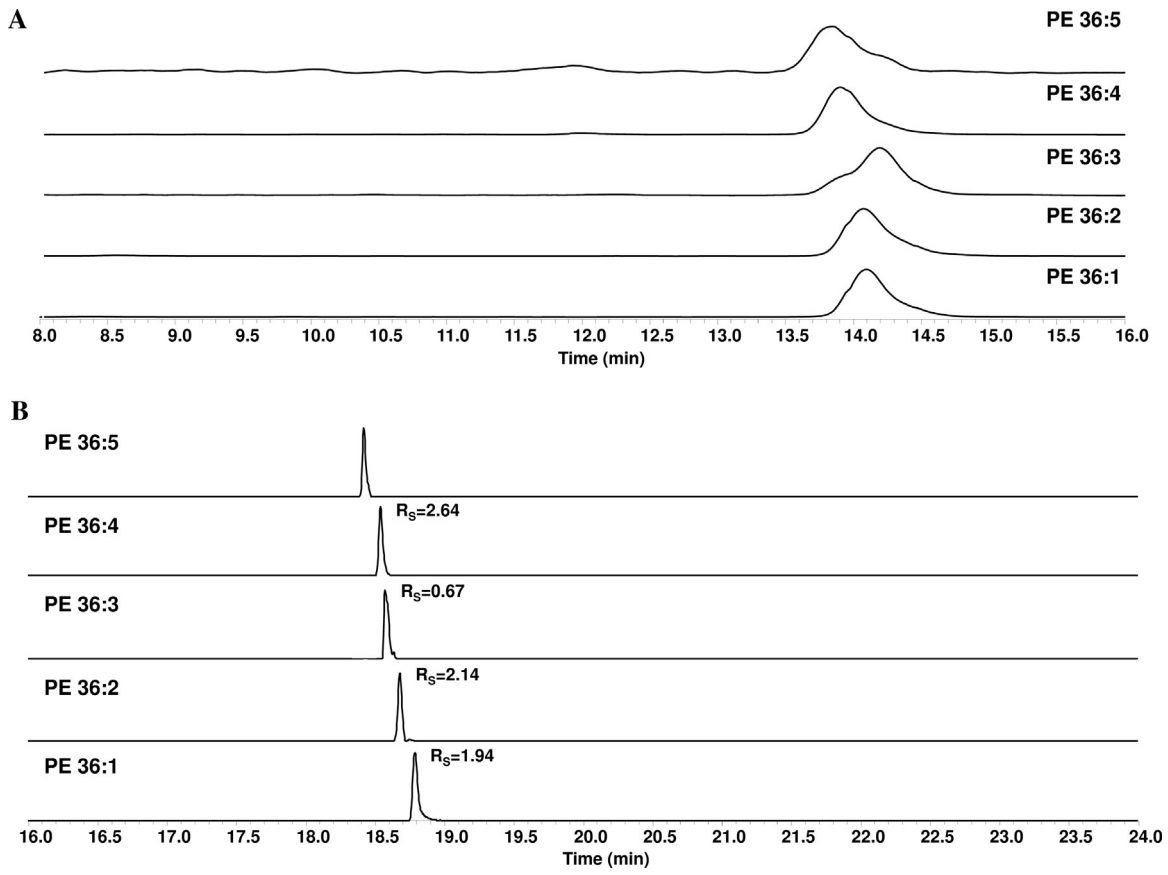

Fig. 3. Extracted ion chromatograms of selected PE species detected by negative mode with 1D-HILIC method (A) and 2D-LC/MS method with obtained chromatographic resolutions (R_S) (B) in VHPC. $R_S = 2 \times (t_{R2}\text{-}t_{R1})/(w_1 + w_2)$.

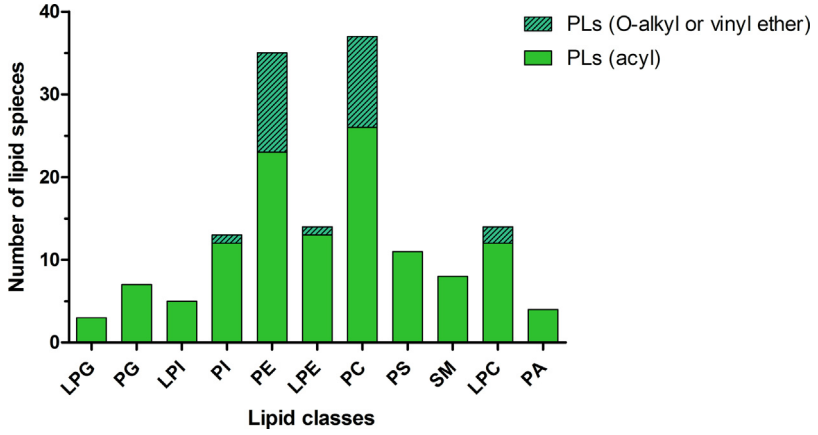

Fig. 4. Identified PL species in mouse brain.

GraphPad Prism 5 (*t*-test) software. At first, by using *t*-test, statistical significances were calculated for the normalized peak areas of lipid classes (sum of normalized peak areas of lipid species in a given class) in nAX and AX brain regions. Significant alterations were observed in four lipid classes and two brain regions. As shown in Fig. S2(A), the normalized peak area of the PE class significantly decreased in VHPC of the AX group. A similar trend was observed for the PS class in PFC; however, in the case of LPG and PA, there was an increase in the normalized peak areas in the AX group compared to those of the nAX group (Fig. S2(B)).

The comparison of normalized peak areas of 151 individual lipid molecules in three brain regions between nAX and AX groups was carried out using multivariate data analysis. Data on Fig. S3(A,C,E) clearly demonstrate the proper separation of nAX and AX mice through the obtained supervised OPLS-DA score plots.

The related S-plots (Fig. S3(B,D,F)) helped to select lipid species, which are present in significantly different concentration in the two groups. Lipid species, which did not differ significantly (dysregulated) in nAX and AX mice, are labeled with green. Lipid species downregulated significantly are located on the lower left section of S-plot, while the upregulated ones are on the upper right section (red dots). S-plots of OPLS-DA methods unveil 37 lipid species with significant differences ($P < 0.05$) between the nAX and AX groups (Fig. S3(B,D,F)).

Table 2
Identified PL species having significantly different concentration in nAX and AX mice.

Mouse brain region	Phospholipid species	Probability	Fold change
DHPC	PE 40:5	<0.001	0.27
DHPC	PE O-36:3, P-36:2	0.011	0.60
DHPC	PE O-38:3, P-38:2	0.017	0.62
DHPC	PE 34:1	0.020	0.84
DHPC	PE O-40:7, P-40:6	0.023	0.75
DHPC	SM 36:1	0.041	1.23
VHPC	PE 40:5	0.001	0.16
VHPC	PC 38:2	0.002	0.56
VHPC	PC O-34:1, P-34:0	0.004	0.58
VHPC	PC 40:2	0.007	0.34
VHPC	PC 40:4	0.009	0.65
VHPC	PC O-36:2, P-36:1	0.010	0.16
VHPC	PE O-40:7, P-40:6	0.013	0.77
VHPC	PE 34:1	0.015	0.78
VHPC	PC 36:3	0.015	0.30
VHPC	PE O-40:8, P-40:7	0.016	0.80
VHPC	PC 38:1	0.020	0.61
VHPC	PE 38:4	0.021	0.79
VHPC	PI 36:5	0.029	0.59
VHPC	PC 40:6	0.030	0.73
VHPC	PE 40:6	0.032	0.84
VHPC	PG 32:0	0.037	0.76
VHPC	PC 38:7, O-38:0	0.037	0.50
VHPC	PC 34:2	0.040	0.76
VHPC	PE O-38:5, P-38:4	0.040	0.79
VHPC	PC O-32:1, P-32:0	0.040	0.65
PFC	PE 40:5	<0.001	3.84
PFC	PE 38:0	0.003	0.24
PFC	PA 40:6	0.006	1.59
PFC	PS 36:1	0.007	0.40
PFC	PA 36:2	0.019	2.21
PFC	PC 42:9	0.019	2.56
PFC	PS 40:6	0.026	0.71
PFC	PE O-38:3, P-38:2	0.031	0.61
PFC	LPE 20:1 (sn-2)	0.031	0.34
PFC	PG 34:2	0.039	1.79
PFC	LPG 18:0	0.042	1.74

PLs and SMs composition of DHPC were compared in nAX and AX groups, too. The results showed that only **SM 36:1** was upregulated, while 5 PEs were found to be downregulated. In particular, **PE 40:5** with the lowest P values had a concentration in AX mice almost 4 times lower (Table 2). Interestingly, **SM 36:1** was the most abundant lipid species compared with other SMs in DHPC, while **PE 40:5** was present in a relatively low concentration (Table S1).

Significantly altered lipid profiles were observed in VHPC of AX mice: 20 lipid species from PE, PC, PI and PG classes were found to be downregulated (in range of 0.16-0.84 fold change) (Table 2).

Fig. 5(A,B) show the mean values with SEM of normalized peak areas of significantly altered polar lipid species from DHPC and VHPC in the nAX and AX groups. In contrast with DHPC, only significant downregulation of VHPC lipid species was observed in mice having elevated anxiety. Again, **PE 40:5** showed the highest concentration differences in the two groups. Similarly, large downregulations were found for **PC O-36:2; P-36:1** (6.25×), **PC 36:3** (3.33×) and **PC 40:2** (2.9×) species (Table 2).

The comparison of normalized peak areas of polar lipids in PFC of nAX and AX mice revealed 11 statistically significant differences

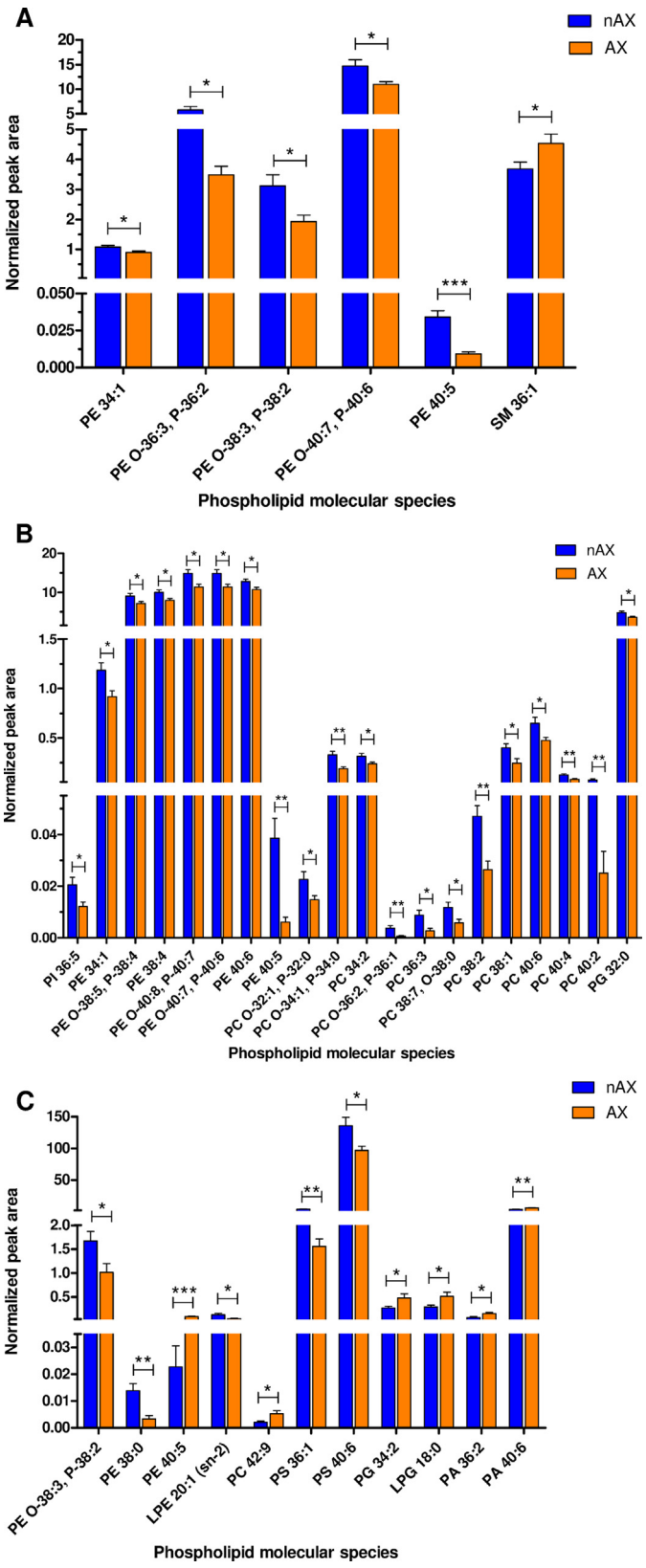

Fig. 5. Normalized peak area of the significantly different PLs of nAX (blue columns) and AX groups (orange columns) in the three brain regions: (A) DHPC, (B) VHPC and (C) PFC. * $P \leq 0.05$; ** $P \leq 0.01$; *** $P \leq 0.001$. (For interpretation of the references to colour in this figure legend, the reader is referred to the web version of this article.)

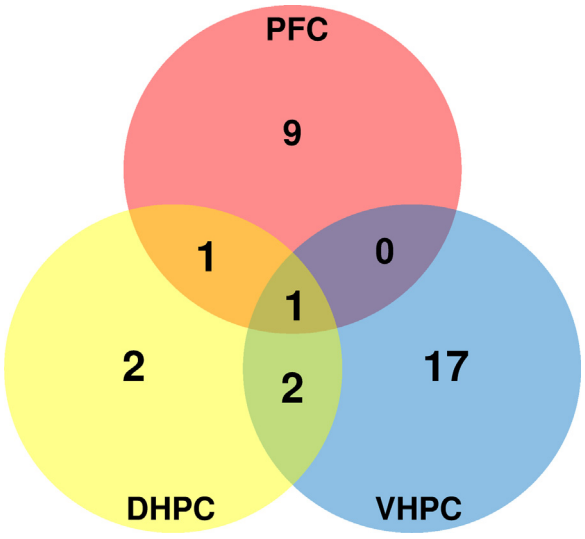

Fig. 6. Distribution of PLs that found to be up- or downregulated in DHPC, VHPC and PFC of AX mice.

in LPE, PE, PC, PS, PG, LPG and PA classes (Table 2, Fig. 5(C)). **PE 38:0**, **PS 36:1**, **PS 40:6, LPE 20:1** and **PE O-38-3**; **PE P-38:2** lipid species were downregulated in PFC of the AX group (Fig. S3(F)). In contrast to DHPC and VHPC, **PE 40:5** was highly upregulated in PCF of the AX mice. Concerning the values of up- and downregulation of lipid species in the AX group, higher than two-fold increases were found for **PE 40:5, PA 36:2** and **PC 42:9**. For **PE 38:0, LPE 20:1 (sn-2)** and **PS 36:1**, in contrast, higher than two-fold decreases were observed.

Table 2 reveals that the majority of PL species having statistically different concentrations in the nAX and AX groups contain unsaturated fatty acids. Furthermore, plasmanyl and plasmenyl PLs exhibiting significant alteration were also present in high percentage.

Finally, Fig. 6 illustrates the distribution of significantly altered PL species in DHPC, VHPC and PFC brain regions of the AX mice. Only **PE 40:5** showed significant alteration in all of the investigated brain regions.

4. Conclusion

This paper describes the development of a comprehensive online 2D-LC/MS method for the analysis of PL and SM species in mouse brain regions. In our novel system, the coupling of HILIC and RP-LC was designed by using two RP trap columns, thus enabled the enrichment of HILIC effluent on the trap column and the separation of the trapped lipids in the second dimension synchronously. In the first dimension, the HILIC separation of lipid classes was divided into five fractions and the analysis of the individual PL and SM species within fractions was performed by four RP runs. The final method provided the quantification of more than 150 PL and SM species in the DHPC, VHPC and PFC brain regions within 40 min run-time. With the established method, the differences of PL composition in brain regions of nAX and AX mice were compared. To our best knowledge, this is the first time that PL and SM alteration of different brain regions in mouse model of anxiety was reported. Our study revealed that 37 PL and SM species had significantly altered concentration in the AX group: 20 were found in VHPC, 6 in DHPC and 11 in PFC. It is worth noting that significant unidirectional alteration of the concentration of PL species was found in VHPC of the AX group. Overall, the developed fully automated 2D method was successfully applied in profiling brain PLs and SMs in mouse model of anxiety disorder.

Acknowledgement

Róbert Berkecz thanks for the financial support of the János Bolyai Research Scholarship of the Hungarian Academy of Sciences.

This research was supported by the EU-funded Hungarian grant EFOP-3.6.1-16-2016-00008.

Appendix A. Supplementary data

Supplementary data associated with this article can be found, in the online version, at https://doi.org/10.1016/j.jpba.2017.10.043.

References

[1] J. Van der Greef, S. Martin, P. Juhasz, A. Adourian, T. Plasterer, E.R. Verheij, R.N. McBurney, The art and practice of systems biology in medicine: mapping patterns of relationships, J. Proteome Res. 6 (2007) 1540–1559.
[2] S. Hanash, Disease proteomics, Nature 422 (2003) 226.
[3] E.A. Dennis, Lipidomics joins the omics evolution, Proc. Natl. Acad. Sci. U. S. A. 106 (2009) 2089–2090.
[4] K. Sandra, A. dos Santos Pereira, G. Vanhoenacker, F. David, P. Sandra, Comprehensive blood plasma lipidomics by liquid chromatography/quadrupole time-of-flight mass spectrometry, J. Chromatogr. A 1217 (2010) 4087–4099.
[5] E. Fahy, S. Subramaniam, R.C. Murphy, M. Nishijima, C.R. Raetz, T. Shimizu, F. Spener, G. van Meer, M.J.O. Wakelam, E.A. Dennis, Update of the LIPID MAPS comprehensive classification system for lipids, J. Lipid Res. 50 (Suppl) (2009) S9–S14.
[6] E. Fahy, M. Sud, D. Cotter, S. Subramaniam, LIPID MAPS online tools for lipid research, Nucleic Acids Res. 35 (Supplement_2) (2007) W606–W612.
[7] X. Han, R.W. Gross, Shotgun lipidomics: electrospray ionization mass spectrometric analysis and quantitation of cellular lipidomes directly from crude extracts of biological samples, Mass Spectrom. Rev. 24 (2005) 367–412.
[8] P.T. Ivanova, S.B. Milne, D.S. Myers, H.A. Brown, Lipidomics: a mass spectrometry based systems level analysis of cellular lipids, Curr. Opin. Chem. Biol. 13 (2009) 526–531.
[9] S. Pati, B. Nie, R.D. Arnold, B.S. Cummings, Extraction, chromatographic and mass spectrometric methods for lipid analysis, Biomed. Chromatogr. 30 (2016) 695–709.
[10] E. Sokol, E. Almeida, H.K. Hannibal-Bach, D. Kotowska, J. Vogt, J. Baumgart, K. Kristiansen, R. Nitsch, J. Knudsen, C.S. Ejsing, Profiling of lipid species by normal-phase liquid chromatography, nanoelectrospray ionization, and ion trap–orbitrap mass spectrometry, Anal. Biochem. 443 (2013) 88–96.
[11] E. Cífková, M. Holčapek, M. Lísa, M. Ovčačíkovaí, F. Lyčka, P. Sandra, Nontargeted quantitation of lipid classes using hydrophilic interaction liquid chromatography–electrospray ionization mass spectrometry with single internal standard and response factor approach, Anal. Chem. 84 (2012) 10064–10070.
[12] H.P. Nguyen, K.A. Schug, The advantages of ESI–MS detection in conjunction with HILIC mode separations: fundamentals and applications, J. Sep. Sci. 31 (2008) 1465–1480.
[13] M. Li, B. Feng, Y. Liang, W. Zhang, Y. Bai, W. Tang, T. Wang, H. Liu, Lipid profiling of human plasma from peritoneal dialysis patients using an improved 2D (NP/RP) LC-QToF MS method, Anal. Bioanal. Chem. 405 (2013) 6629–6638.
[14] Y.S. Ling, H.J. Liang, M.H. Lin, C.H. Tang, K.Y. Wu, M.L. Kuo, C.Y. Lin, Two-dimensional LC–MS/MS to enhance ceramide and phosphatidylcholine species profiling in mouse liver, Biomed. Chromatogr. 28 (2014) 1284–1293.
[15] J.F. Li, X. Yan, Y.L. Wu, M.J. Fang, Z. Wu, Y.K. Qiu, Comprehensive two-dimensional normal-phase liquid chromatography × reversed-phase liquid chromatography for analysis of toad skin, Anal. Chim. Acta 962 (2017) 114–120.
[16] M. Holčapek, M. Ovčačíková, M. Lísa, E. Cífková, T. Hájek, Continuous comprehensive two-dimensional liquid chromatography–electrospray ionization mass spectrometry of complex lipidomic samples, Anal. Bioanal. Chem. 407 (2015) 5033–5043.
[17] Y. Shan, Y. Liu, L. Yang, H. Nie, S. Shen, C. Dong, Y. Bai, Q. Sun, J. Zhao, H. Liu, Lipid profiling of cyanobacteria Synechococcus sp. PCC 7002 using two-dimensional liquid chromatography with quadrupole time-of-flight mass spectrometry, J. Sep. Sci. 39 (2016) 3745–3753.
[18] S. Wang, X. Shi, G. Xu, Online three dimensional liquid chromatography/mass spectrometry method for the separation of complex samples, Anal. Chem. 89 (2017) 1433–1438.
[19] M. Lísa, E. Cífková, M. Holčapek, Lipidomic profiling of biological tissues using off-line two-dimensional high-performance liquid chromatography?mass spectrometry, J. Chromatogr. A 1218 (2011) 5146–5156.
[20] M. Li, X. Tong, P. Lv, B. Feng, L. Yang, Z. Wu, X. Cui, Y. Bai, Y. Huang, H. Liu, A not-stop-flow online normal-/reversed-phase two-dimensional liquid chromatography–quadrupole time-of-flight mass spectrometry method for comprehensive lipid profiling of human plasma from atherosclerosis patients, J. Chromatogr. A 1372 (2014) 110–119.

[21] D.R. Stoll, Recent advances in 2D-LC for bioanalysis, Bioanalysis 7 (2015) 3125–3142.
[22] M.A. Parent, L. Wang, J. Su, T. Netoff, L.L. Yuan, Identification of the hippocampal input to medial prefrontal cortex in vitro, Cereb. Cortex 20 (2009) 393–403.
[23] R.W.H. Verwer, R.J. Meijer, H.F.M. Van Uum, M.P. Witter, Collateral projections from the rat hippocampal formation to the lateral and medial prefrontal cortex, Hippocampus 7 (1997) 397–402.
[24] S. Adhikari, M.A. Topiwala, J.A. Gordon, Single units in the medial prefrontal cortex with anxiety-related firing patterns are preferentially influenced by ventral hippocampal activity, Neuron 71 (2011) 898–910.
[25] A. Adhikari, M.A. Topiwala, J.A. Gordon, Synchronized activity between the ventral hippocampus and the medial prefrontal cortex during anxiety, Neuron 65 (2010) 257–269.
[26] L. Jacobson, R. Sapolsky, The role of the hippocampus in feedback regulation of the hypothalamic-pituitary-adrenocortical axis, Endocr. Rev. 12 (1991) 118–134.
[27] N. Maggio, M. Segal, Differential corticosteroid modulation of inhibitory synaptic currents in the dorsal and ventral hippocampus, J. Neurosci. 29 (2009) 2857–2866.
[28] A. Pitkänen, M. Pikkarainen, N. Nurminen, A. Ylinen, Reciprocal connections between the amygdala and the hippocampal formation, perirhinal cortex, and postrhinal cortex in rat: a review, Ann. N. Y. Acad. Sci. 911 (2000) 369–391.
[29] A. Albrecht, G. Çalışkan, M.S. Oitzl, U. Heinemann, O. Stork, Long-lasting increase of corticosterone after fear memory reactivation: anxiolytic effects and network activity modulation in the ventral hippocampus, Neuropsychopharmacology 38 (2013) 386.
[30] É.M. Szegő, T. Janáky, Z. Szabó, A. Csorba, H. Kompagne, G. Müller, G. Lévay, A. Simor, G. Juhász, K.A. Kékesi, A mouse model of anxiety molecularly characterized by altered protein networks in the brain proteome, Eur. Neuropsychopharmacol. 20 (2010) 96–111.
[31] J. Horváth, T. Szögi, G. Müller, V. Szegedi, The anxiolytic buspirone shifts coping strategy in novel environmental context of mice with different anxious phenotype, Behav. Brain Res. 250 (2013) 32–38.
[32] J. Folch, M. Lees, G.H. Sloane-Stanley, A simple method for the isolation and purification of total lipids from animal tissues, J. Biol. Chem. 226 (1957) 497–509.
[33] T. Kind, K.H. Liu, D.Y. Lee, B. DeFelice, J.K. Meissen, O. Fiehn, LipidBlast in silico tandem mass spectrometry database for lipid identification, Nat. Methods 10 (2013) 755–758.
[34] L. Abdullah, J.E. Evans, S. Ferguson, B. Mouzon, H. Montague, J. Reed, G. Crynen, T. Emmerich, M. Crocker, R. Pelot, M. Mullan, F. Crawford, Lipidomic analyses identify injury-specific phospholipid changes 3 mo after traumatic brain injury, FASEB J. 28 (2014) 5311–5321.
[35] C. Bascoul-Colombo, I.A. Guschina, B.H. Maskrey, M. Good, V.B. O'Donnell, J.L. Harwood, Dietary DHA supplementation causes selective changes in phospholipids from different brain regions in both wild type mice and the Tg2576 mouse model of Alzheimer's disease, Biochim. Biophys. Acta Mol. Cell. Biol. Lipids 1861 (2016) 524–537.
[36] S.M. van Liempd, D. Cabrera, F.Y. Lee, E. González, E.C. Dell'Angelica, C.A. Ghiani, J.M. Falcon-Perez, BLOC-1 deficiency causes alterations in amino acid profile and in phospholipid and adenosine metabolism in the postnatal mouse hippocampus, Sci. Rep. 7 (2017) 1–11.
[37] T.G. Oliveira, R.B. Chan, F.V. Bravo, A. Miranda, R.R. Silva, B. Zhou, F. Marques, V. Pinto, J.J. Cerqueira, G. Di Paolo, N. Sousa, The impact of chronic stress on the rat brain lipidome, Mol. Psychiatry. 21 (2016) 80.
[38] C.H. Cortie, A.J. Hulbert, S.E. Hancock, T.W. Mitchell, D. McAndrew, P.L. Else, Of mice, pigs and humans: an analysis of mitochondrial phospholipids from mammals with very different maximal lifespans, Exp. Gerontol. 70 (2015) 135–143.
[39] T. Zhang, S. Chen, X. Liang, H. Zhang, Development of a mass-spectrometry-based lipidomics platform for the profiling of phospholipids and sphingolipids in brain tissues, Anal. Bioanal. Chem. 407 (2015) 6543–6555.
[40] A.J. Alpert, Hydrophilic-interaction chromatography for the separation of peptides, nucleic acids and other polar compounds, J. Chromatogr. A 499 (1990) 177–196.
[41] P. Hemström, K. Irgum, Hydrophilic interaction chromatography, J. Sep. Sci. 29 (2006) 1784–1821.
[42] B.K. Matuszewski, M.L. Constanzer, C.M. Chavez-Eng, Strategies for the assessment of matrix effect in quantitative bioanalytical methods based on HPLC-MS/MS, Anal. Chem. 75 (2003) 3019–3030.
[43] H. Trufelli, P. Palma, G. Famiglini, A. Cappiello, An overview of matrix effects in liquid chromatography–mass spectrometry, Mass Spectrom. Rev. 30 (2011) 491–509.
[44] N.E. Braverman, A.B. Moser, Functions of plasmalogen lipids in health and disease, Biochim. Biophys. Acta Mol. Basis Dis. 1822 (2012) 1442–1452.